Conductive Properties of the Proximal Tubule in *Necturus* Kidney

T. ANAGNOSTOPOULOS, J. TEULON, and A. EDELMAN

From the Unité de Recherche sur les Maladies du Métabolisme chez l'Enfant (U-192), Institut National de la Santé et de la Recherche Médicale, Hôpital Necker Enfants-Malades and Centre National de la Recherche Scientifique GRECO, 75730 Paris, France

ABSTRACT The electrical properties of the proximal tubule of the in vivo *Necturus* kidney were investigated by injecting current (as rectangular waves) into the lumen or into the epithelium of single tubules and by studying the resulting changes of transepithelial (V_L) and/or cell membrane potential (V_C) at various distances from the source. In some experiments paired measurements of V_L and V_C were performed at two abscissas x and x'. The luminal length constant of about 1,030 μm was shown to provide a good estimate of the transepithelial resistance, specific resistance (R_{TE} = 420 $\Omega \cdot cm^2$) and/or per unit length (r_{TE} = 1.3 × 10^4 $\Omega \cdot cm$). The apparent intraepithelial length constant was subject to distortions arising from concomitant current spread in the lumen. The resistances of luminal membrane (r_L), basolateral membrane (r_B), and shunt pathway (r_S) were estimated by two independent methods at 3.5 × 10^4, 1.2 × 10^4, and 1.7 × 10^4 $\Omega \cdot cm$, respectively. The corresponding specific resistances were close to 1,200, 600, and 600 $\Omega \cdot cm^2$. There are two main conclusions of this study. (*a*) The resistances of cell membranes and shunt pathway are of the same order of magnitude. The figure of the shunt resistance is at variance with the notion that the proximal tubule of *Necturus* is a leaky epithelium. (*b*) A rigorous assessment of the conductive properties of concentric cylindrical double cables (such as renal tubules) requires that electrical interactions arising from one cable to another be taken into account. Appropriate equations were developed to deal with this problem.

INTRODUCTION

A quantitative evaluation of the three main resistances of the proximal tubule in *Necturus* is of primary importance to our eventual understanding of transepithelial ion transport. Several studies have been devoted to this subject in the past. However, in spite of considerable work, a number of questions remain still unanswered. The reasons that prompted us to reassess the conductive properties of the amphibian proximal tubule are threefold. (*a*) The initial estimate of the in vivo transepithelial specific resistance R_{TE} = 650 $\Omega \cdot cm^2$ (29) was questioned in subsequent work in which it was suggested that R_{TE} was about 40–70 $\Omega \cdot cm^2$ (7, 26, 28). However, other studies of the in vitro preparation produced higher estimates, ranging from 250 to 430 $\Omega \cdot cm^2$

J. GEN. PHYSIOL. © The Rockefeller University Press · 0022-1295/80/05/0553/35 $1.00 553
Volume 75 May 1980 553–587

(9, 19). (*b*) No attempt has been made to determine separately cell membrane resistances, luminal and/or peritubular. Their sum in series, R_{TC}, has been assessed in the in vivo (29) and in the perfused (4) *Necturus* kidney. However, the technique used in those studies is suitable to measure the sum of cell membrane resistances in parallel, R_{PAR}, not their sum in series R_{TC} (4). Thus, the reported estimates of R_{TC} ought to be reassessed by more appropriate techniques. (*c*) The proximal tubule of *Necturus*, like other renal epithelia, is made up of two concentric cables, luminal and epithelial. Injection of current into one of the two cables, via a point source, may produce significant leaks of current into the companion cable especially near the source where current density is maximal. As a result, current will flow longitudinally not only along the cable containing the actual source, but also along its companion cable. In addition, current will flow from one cable to another in the transverse direction, if there are transverse voltage gradients; the magnitude of such interactions will be essentially a function of the conductive properties of the two cables. Under certain circumstances one may anticipate the fraction of current leaking from one cable to another to change in magnitude and, possibly, in direction with distance from the source, altering accordingly the pattern of voltage attenuation at least in the cable with the smaller "intrinsic" length constant. Clearly, the situations that may be encountered in concentric double cables may vary widely; they cannot be dealt with adequately by such simple and intuitive considerations. A theoretical framework, in which voltage distribution along each cable is described, by taking into account cable-to-cable interactions, is necessary; such an analysis is useful, not only for the proximal tubule of *Necturus* but also for future experimental studies in renal tubules.

MAIN SYMBOLS AND NOTATIONS

The specific transverse resistances ($\Omega \cdot cm^2$) of the conductive barriers of the proximal tubule are designated by R and appropriate subscripts:

R_A resistance of the apical (luminal) membrane
R_B resistance of the basolateral (peritubular) membrane
R_S resistance of the shunt pathway
R_{TC} transcellular resistance; $R_{TC} = R_B + R_A$
R_{TE} transepithelial resistance; $R_{TE} = R_{TC} R_S/(R_{TC} + R_S)$
R_Z sum of the luminal membrane resistance plus the shunt resistance in series; $R_Z = R_A + R_S$
R_{PAR} sum in parallel of the two resistive limbs, R_B plus R_Z, connecting the cell interior with the interstitium; $R_{PAR} = R_B R_Z/(R_B + R_Z)$.

Specific resistances are expressed per apparent surface area; i.e., peritubular and luminal membrane areas are calculated from outside and inside tubular diameters, respectively. Lateral cell membrane area is neglected in the computation of R_B.

The above resistances may be expressed as transverse resistances per unit length, r ($\Omega \cdot cm$) or as specific conductances G (mho/cm^2); the same subscripts are used. In addition:

α luminal radius (cm)

β thickness of the epithelial layer (cm)
x distance from the source (cm)
θ_L specific resistivity of the luminal fluid (Ω·cm)
θ_C specific resistivity of the epithelial cable (Ω·cm)
ρ_L, ρ_C core resistance of lumen and epithelial cable, respectively, per unit length (Ω/cm)
I, i current (A) and linear current density (A/cm) in longitudinal and transverse directions respectively; subscripts A, B, S, L, and C are as above; I_0 is the injected current
V change in potential (volts) consecutive to current injection at the source; V_L will indicate the transepithelial electrotonic potential (lumen minus interstitium); V_C will be the cell (electrotonic) potential with reference to interstitium

λ_L and λ_C (cm) are the length constants of luminal and epithelial cables respectively, defined for each cable only by the resistances of its limiting barriers: cable-to-cable interactions are not taken into account. The mathematical definition of λ_L and λ_C is given in the theoretical section. λ_D and λ_E (cm) are the length constants of luminal and epithelial (cell) cables, respectively, describing voltage distribution along each cable by taking into account the resistive properties of both the cable under consideration and its companion cable. The detailed mathematical expressions of λ_D and λ_E are given in the following section (Eqs. 16*a* and 16*b*). λ_{LM} and λ_{CM} (cm) are the experimentally determined or "apparent" length constants of luminal and cell cables, respectively. A second subscript, c or l, indicates source localization; e.g., λ_{LM_c} is the measured luminal length constant obtained with an intraepithelial point source.

THEORETICAL CONSIDERATIONS

This section deals with voltage distribution along both luminal and intraepithelial cables, following injection of current through a point source, luminal or intraepithelial. Our purpose in this section is not to undertake an exhaustive analysis of voltage distribution in concentric cylindrical cables. We wish, rather, to consider the non-Besselian portion of the voltage attenuation curve in each cable, by focusing on the peculiarities arising from cable to cable interactions. We shall neglect the initial portion of the epithelial cable in which circumferential current density is not uniform (4, 25) and that of the luminal cable in which radial distortions are likely to occur near the source, as in other ordinary cables. The mathematical treatment of electrical interactions at the initial part of the companion cables is too complex and of limited practical interest, since an experimental determination of circumferential voltage gradients in the epithelial cable and/or axial voltage gradients in the lumen is hardly imaginable with present techniques in renal tubules. The initial portion not to be considered, may be estimated for all practical purposes to be smaller than $2\pi\alpha$ (4). Beyond that point, the electrical variables will be expressed as a function of distance x from the source.

The assumptions inherent in this analysis are: (*a*) The cellular layer is assumed to be a regular hollow cylinder of uniform resistivity, uniform

thickness, and infinite length, the luminal core being a regular cylinder of uniform resistivity and infinite length. The electrical equivalent of the proximal tubule may be then conceived of as a series of elementary circuits such as the circuit represented in Fig. 1. (*b*) The external medium is supposed to be infinitely conductive. (*c*) The increase in surface area of peritubular and luminal membranes by cell infoldings and brush border appearance, respectively, are neglected. (*d*) The tip of the stimulating electrode is assumed to be reduced to a single point. (*e*) Only the steady-state potential achieved during current injection is considered; membrane capacities are neglected.

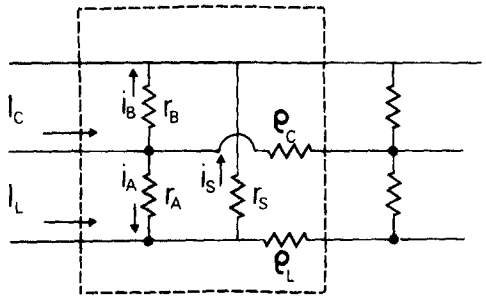

FIGURE 1. An equivalent electrical circuit used to study current and voltage distribution along the length of cylindrical concentric cables, by taking into account electrical interactions arising from luminal to epithelial cable and/or vice versa. The elementary unit is limited by the dashed line. The source may be in the lumen or in the epithelium. I_C and I_L designate flow of current along the longitudinal axis of the tubule. i_B, i_A, and i_S are radial current flow. ρ_C and ρ_L are the core resistivities of the epithelial and luminal cables, respectively; r_B, r_A, and r_S are the resistances (per unit length) of the basolateral membrane, apical membrane, and shunt pathway, respectively.

General Description of Voltage Attenuation along the Companion Luminal and Epithelial Cables

Voltage and current distribution within the elementary unit of the circuit shown in Fig. 1 is given by Ohm's law, used in the differential form

$$\left(\frac{dV_L}{dx}\right)_x = -\rho_L(I_L)_x; \tag{1}$$

$$\left(\frac{dV_C}{dx}\right)_x = -\rho_C(I_C)_x, \tag{2}$$

where the subscript x indicates the value of the various functions and parameters at abscissa x. Further, from Kirchhoff's law we obtain

$$\left(\frac{dI_L}{dx}\right)_x = -(i_S)_x + (i_A)_x; \tag{3}$$

$$\left(\frac{dI_C}{dx}\right)_x = -(i_A)_x - (i_B)_x. \tag{4}$$

According to Ohm's law

$$(V_L)_x = r_S(i_S)_x; \tag{5}$$

$$(V_C)_x = r_B(i_B)_x; \tag{6}$$

$$(V_C - V_L)_x = r_A(i_A)_x. \tag{7}$$

By differentiating Eq. 1 and combining with Eq. 3 we obtain

$$\frac{d^2V_L}{dx^2} = -\rho_L \frac{dI_L}{dx} = \rho_L(i_S - i_A), \tag{8}$$

which, together with Eqs. 5 and 6, yields

$$\frac{d^2V_L}{dx^2} = \rho_L \left(\frac{V_L}{r_S} + \frac{V_L - V_C}{r_A}\right). \tag{9}$$

Setting

$$\frac{1}{r_S} + \frac{1}{r_A} = \frac{1}{r_{SA}},$$

Eq. 9 may be rewritten, after rearrangement

$$\frac{d^2V_L}{dx^2} - \frac{V_L\rho_L}{r_{SA}} = -\frac{V_C\rho_L}{r_A}. \tag{10 a}$$

Similarly, by setting

$$\frac{1}{r_B} + \frac{1}{r_A} = \frac{1}{r_{BA}},$$

differentiation of Eq. 2 leads to

$$\frac{d^2V_C}{dx^2} - \frac{V_C\rho_C}{r_{BA}} = -\frac{V_L\rho_C}{r_A}. \tag{11a}$$

We define

$$\lambda_L^2 = r_{SA}/\rho_L,$$
$$\lambda_C^2 = r_{BA}/\rho_C,$$
$$\gamma_L = \rho_L/r_A,$$
$$\gamma_C = \rho_C/r_A.$$

Then, Eqs. 10 a and 11 a may be rewritten

$$\frac{d^2V_L}{dx^2} - \frac{1}{\lambda_L^2} V_L = -\gamma_L V_C, \tag{10b}$$

and

$$\frac{d^2V_C}{dx^2} - \frac{1}{\lambda_C^2} V_C = -\gamma_C V_L, \tag{11b}$$

By differentiating twice Eq. 10 b and combining then with Eq. 11 b, we obtain

after rearrangement

$$\frac{d^4V_L}{dx^4} - \frac{d^2V_L}{dx^2}\left(\frac{1}{\lambda_L^2} + \frac{1}{\lambda_C^2}\right) + \left(\frac{1}{\lambda_L^2\lambda_C^2} - \gamma_L\gamma_C\right)V_L = 0. \tag{12a}$$

A similar procedure yields

$$\frac{d^4V_C}{dx^4} - \frac{d^2V_C}{dx^2}\left(\frac{1}{\lambda_L^2} + \frac{1}{\lambda_C^2}\right) + \left(\frac{1}{\lambda_L^2\lambda_C^2} - \gamma_L\gamma_C\right)V_C = 0. \tag{12b}$$

The general solution to the Eqs. 12 *a* and 12 *b* is a linear system of four exponential terms, $e^{\xi x}$; the coefficients ξ in the exponent are defined by

$$\xi^4 - \left(\frac{1}{\lambda_L^2} + \frac{1}{\lambda_C^2}\right)\xi^2 + \left(\frac{1}{\lambda_L^2\lambda_C^2} - \gamma_L\gamma_C\right) = 0. \tag{13}$$

Thus we get

$$\xi^2 = \frac{1}{2}\left\{\frac{1}{\lambda_L^2} + \frac{1}{\lambda_C^2} \pm \left[\left(\frac{1}{\lambda_C^2} - \frac{1}{\lambda_L^2}\right)^2 + 4\gamma_L\gamma_C\right]^{1/2}\right\}. \tag{14}$$

1 129

The condition, necessary to obtain four real solutions for ξ is $\xi^2 > 0$; i.e.,

$$\frac{1}{\lambda_L^2} + \frac{1}{\lambda_C^2} > \left[\left(\frac{1}{\lambda_C^2} + \frac{1}{\lambda_L^2}\right)^2 + 4\left(\gamma_L\gamma_C - \frac{1}{\lambda_L^2\lambda_C^2}\right)\right]^{1/2}, \tag{15a}$$

and thus

$$\gamma_L\gamma_C - \frac{1}{\lambda_L^2\lambda_C^2} < 0 \tag{15b}$$

or

$$\frac{\rho_L\rho_C}{r_{SA}r_{BA}} > \frac{\rho_L\rho_C}{r_A^2}. \tag{15c}$$

The condition set by Eq. 15 *c* is met since, by definition, r_{SA}, $r_{BA} < r_A$. Hence, there are four real solutions to Eq. 13, given by Eq. 14. However, the boundary condition $V_\infty = 0$ requires that the two solutions introducing positive exponential terms in the solutions of Eqs. 12 *a* and 12 *b* must be discarded. The remaining solutions are

$$\xi = -\frac{1}{\sqrt{2}}\left\{\frac{1}{\lambda_L^2} + \frac{1}{\lambda_C^2} \pm \left(\frac{1}{\lambda_C^2} - \frac{1}{\lambda_L^2}\right)(1 + m)^{1/2}\right\}^{1/2}, \tag{16}$$

where

$$m = 4\gamma_L\gamma_C \Big/ \left(\frac{1}{\lambda_C^2} - \frac{1}{\lambda_L^2}\right)^2. \tag{17}$$

We shall define the two solutions of Eq. 13 as $-1/\lambda_E$ and $-1/\lambda_D$, which after

rearrangement yield

$$\frac{1}{\lambda_E^2} = \frac{1}{\lambda_C^2}\,\frac{1 + (1 + m)^{1/2}}{2} + \frac{1}{\lambda_L^2}\,\frac{1 - (1 + m)^{1/2}}{2} \tag{16a}$$

and

$$\frac{1}{\lambda_D^2} = \frac{1}{\lambda_L^2}\,\frac{1 + (1 + m)^{1/2}}{2} + \frac{1}{\lambda_C^2}\,\frac{1 - (1 + m)^{1/2}}{2}. \tag{16b}$$

Using these notations, the general solutions of Eqs. 12 *a* and 12 *b* are

$$V_L = K_L\, e^{-x/\lambda_E} + K'_L\, e^{-x/\lambda_D}; \tag{18a}$$

$$V_C = K_C\, e^{-x/\lambda_E} + K'_C\, e^{-x/\lambda_D}. \tag{18b}$$

Determination of the Constants K_C, K'_C, K_L, K'_L

The next step in this analysis will be the query to determine the above constants from boundary conditions, which may be expressed in general terms as

$$\left(\frac{dV_C}{dx}\right)_{x=0} = S_C; \tag{19a}$$

$$\left(\frac{dV_L}{dx}\right)_{x=0} = S_L. \tag{19b}$$

By introducing the values of V_L, V_C (see Eqs. 18 *a* and 18 *b*) in Eqs. 10 *b* or 11 *b*, and further combining with the boundary conditions 19 *a* and 19 *b*, we obtain

$$\frac{K_C}{\lambda_E}\left(\frac{1}{\lambda_E^2} - \frac{1}{\lambda_C^2}\right) + \frac{K'_C}{\lambda_D}\left(\frac{1}{\lambda_D^2} - \frac{1}{\lambda_C^2}\right) = S_L \gamma_C; \tag{19c}$$

$$\frac{K_C}{\lambda_E} + \frac{K'_C}{\lambda_D} = -S_C. \tag{19d}$$

Similarly, K_L and K'_L are given by

$$K_L = -\left(\frac{1}{\lambda_E^2} - \frac{1}{\lambda_C^2}\right)\frac{K_C}{\gamma_C}; \tag{19e}$$

$$K'_L = -\left(\frac{1}{\lambda_D^2} - \frac{1}{\lambda_C^2}\right)\frac{K'_C}{\gamma_C}. \tag{19f}$$

Determination of the Constants K in Specific Situations

We shall assume each cable of the proximal tubule not to display radial gradients of current; i.e., only unidimensional coupling between the cables

will be considered. In addition, it is pointed out that voltage attenuation is a continuous function of distance x in each cable; i.e., there is no break point along the whole length unless the tubule becomes damaged. The transverse flows of current i_A, i_B, i_S (in amperes per centimeter) are also continuous functions of x: they can be defined only with regard to a given distance dx. Each of those currents i results in the decrease of a longitudinal current I (in amperes); for this reason, the value of I is also defined at an abscissa x. Thus, from Eqs. 3 and 4 we obtain

$$dI_L = (-i_S + i_A)\,dx; \tag{3a}$$

$$dI_C = (-i_A - i_B)\,dx. \tag{4a}$$

Obviously the change in longitudinal current (dI) tends towards zero when $dx \to 0$.

INTRAEPITHELIAL INJECTION OF CURRENT In this experimental situation, in addition to the intraepithelial current injecting microelectrode, two recording tips are inserted in the lumen and the epithelium, respectively, at a single abscissa x. At $x = 0$ the injected current I_0 is equally divided along the x axis; i.e., the current delivered at each half-cable is $I_0/2$; the longitudinal current at $x = 0$ is

$$(I_C)_{x=0} = I_0/2.$$

Although current density is very high at the source, no decrease dI_C of I_C will occur before an elementary distance dx (Eq. 4 *a*). At the same distance dx, the transverse flow of current $-i_A dx$ gives rise to the longitudinal current I_L, but at $x = 0$ no such current may arise; i.e., $(I_L)_{x=0} = 0$.
Thus, the boundary conditions[1]:

$$\left(\frac{dV_C}{dx}\right)_{x=0} = -\rho_C \frac{I_0}{2}; \tag{20a}$$

$$\left(\frac{dV_L}{dx}\right)_{x=0} = 0. \tag{20b}$$

[1] We arrive at the same conclusion by integrating the transverse flows of current:

$$\int_0^\infty (i_A + i_B)\,dx = I_0/2;$$

$$\int_0^\infty i_A\,dx = \int_0^\infty i_S\,dx.$$

Using a luminal source, we have

$$\int_0^\infty (-i_S + i_A)\,dx = I_0/2;$$

$$\int_0^\infty (-i_A)\,dx = \int_0^\infty i_B\,dx.$$

The solution of Eqs. 19 *a*–19 *f* yields

$$K_C = \frac{\rho_C I_0}{4} \lambda_E [1 + (1 + m)^{-1/2}]; \tag{21a}$$

$$K'_C = \frac{\rho_C I_0}{4} \lambda_D [1 - (1 + m)^{-1/2}]; \tag{21b}$$

$$-\frac{K_L}{\lambda_E} = \frac{K'_L}{\lambda_D} = \frac{\rho_C I_0}{2} \frac{\gamma_L}{\frac{1}{\lambda_C^2} - \frac{1}{\lambda_L^2}} (1 + m)^{-1/2}. \tag{21c}$$

INTRALUMINAL INJECTION OF CURRENT In this case the current-injecting tip is intraluminal; the recording microelectrodes are set as above. A similar line of argument yields the boundary conditions

$$\left(\frac{dV_C}{dx}\right)_{x=0} = 0; \tag{22a}$$

$$\left(\frac{dV_L}{dx}\right)_{x=0} = -\rho_L \frac{I_0}{2}. \tag{22b}$$

They allow an estimate of the coefficients K (see Eqs. 19 *a*–19 *f*):

$$-\frac{K_C}{\lambda_E} = \frac{K'_C}{\lambda_D} = \frac{\rho_L I_0}{2} \frac{\gamma_C}{\frac{1}{\lambda_C^2} - \frac{1}{\lambda_L^2}} (1 + m)^{-1/2}; \tag{23a}$$

$$K_L = \frac{\rho_L I_0}{4} \lambda_E [1 - (1 + m)^{-1/2}]; \tag{23b}$$

$$K'_L = \frac{\rho_L I_0}{4} \lambda_D [1 + (1 + m)^{-1/2}]. \tag{23c}$$

Summary of the General Solutions Describing Voltage Distribution in the Companion Luminal and Epithelial Cables: the Source Is Alternatively Considered in Epithelium and Lumen

Upon intraepithelial injection of current, voltage attenuation along the companion epithelial and luminal cables is given respectively by

$$V_C = \frac{\rho_C I_0}{4} \{[1 + (1 + m)^{-1/2}]\lambda_E e^{-x/\lambda_E} + [1 - (1 + m)^{-1/2}]\lambda_D e^{-x/\lambda_D}\}; \tag{24a}$$

$$V_L = \frac{\rho_C I_0}{2} \frac{\gamma_L}{\frac{1}{\lambda_C^2} - \frac{1}{\lambda_L^2}} (1 + m)^{-1/2}[-\lambda_E e^{-x/\lambda_E} + \lambda_D e^{-x/\lambda_D}]. \tag{24b}$$

Intraluminal injection of current yields the following pattern

$$V_C = \frac{\rho_L I_0}{2} \frac{\gamma_C}{\frac{1}{\lambda_C^2} - \frac{1}{\lambda_L^2}} (1 + m)^{-1/2}[-\lambda_E e^{-x/\lambda_E} + \lambda_D e^{-x/\lambda_D}]; \tag{25a}$$

$$V_L = \frac{\rho_L I_0}{4}\{[1-(1+m)^{-1/2}]\lambda_E e^{-x/\lambda_E} + [1+(1+m)^{-1/2}]\lambda_D e^{-x/\lambda_D}\}. \quad (25\,b)$$

Simplification of the Above General Equations (Solutions), Applied to the Proximal Tubule of Necturus

TWO BASIC ASSUMPTIONS Eqs. 24 *a*, 24 *b*, 25 *a*, and 25 *b* describe the general form of voltage attenuation in epithelial and luminal cables. When applied to the proximal tubule of *Necturus* they may be simplified, provided that pertinent experimental observations are taken into account. At this point we shall make the following two assumptions:

$$\lambda_E e^{-x/\lambda_E} \ll \lambda_D e^{-x/\lambda_D}; \quad (26)$$

$$\lambda_E^2/\lambda_D^2 \ll 1. \quad (27)$$

These assumptions stem from consideration of and are consistent with the data of this work. They will be justified on experimental grounds in the Results section (see Footnotes 4 and 5). They yield a third inequality[2]:

$$m/4 \ll 1 \quad (28)$$

AN ESTIMATE OF λ_E AND OF λ_D Using the MacLaurin expansion method and recalling inequality 1 *F* in Footnote 1, Eq.16 *a* is simplified to

$$\frac{1}{\lambda_E^2} = \frac{1}{\lambda_C^2}\left[1+\frac{m}{4}\left(1-\frac{\lambda_C^2}{\lambda_L^2}\right)\right] \simeq \frac{1}{\lambda_C^2}\left(1+\frac{m}{4}\right). \quad (29)$$

Further use of the MacLaurin series leads to

$$\frac{1}{\lambda_E} \simeq \frac{1}{\lambda_C}\left(1+\frac{m}{8}\right).$$

Since $m/4 \ll 1$ (see inequality28), we may write

$$\lambda_E \simeq \lambda_C \quad (30)$$

On the other hand, applying the MacLaurin expansion treatment to Eq. 16 *b* and recalling inequality 28, we obtain

$$\frac{1}{\lambda_D^2} = \frac{1}{\lambda_L^2}\left(1+\frac{m}{4}-\frac{m}{4}\frac{\lambda_L^2}{\lambda_C^2}\right) \simeq \frac{1}{\lambda_L^2}\left(1-\frac{m}{4}\frac{\lambda_L^2}{\lambda_C^2}\right). \quad (31)$$

[2] From assumption 27 and Eqs. 16 *a* and 16 *b* we obtain

$$1/\lambda_C^2 \gg 1/\lambda_L^2. \quad (1\,F)$$

Since by definition $\gamma_L < 1/\lambda_L^2$ and $\gamma_C < 1/\lambda_C^2$, the inequality 1 *F* yields

$$\gamma_L\gamma_C\lambda_L^2\lambda_C^2 < 1. \quad (2\,F)$$

From 1 *F* and 2 *F*, it is obvious that

$$\gamma_L\gamma_C\lambda_C^4 \ll \gamma_L\gamma_C\lambda_L^2\lambda_C^2 < 1. \quad (3\,F)$$

Combination of 1 *F*, 3 *F*, and Eq. 17 leads to inequality 28.

VOLTAGE ATTENUATION ALONG CELLULAR AND LUMINAL CABLES: SIMPLIFIED EQUATIONS EXPRESSED AS A FUNCTION OF RESISTANCES PER UNIT LENGTH Recalling that $m/4 \ll 1$ and applying the MacLaurin power expansion treatment to the coefficients of Eqs. 24 *a*, 24 *b*, 25 *a*, 25 *b*, the following simplifications are obtained: $1 + (1 + m)^{-1/2} \simeq 2$; $1 - (1 + m)^{-1/2} \simeq m/2$; $(1 + m)^{-1/2} \simeq 1$. As a result, the Eqs. 24 *a*, 24 *b*, 25 *a*, and 25 *b* are also simplified. They are given hereafter in their reduced form in which the functions V_L and V_C are expressed in terms of membrane resistances and core resistivities per unit of tubular length.

Luminal Injection of Current Intraepithelial voltage attenuation is given by

$$V_C = \frac{\rho_L I_0}{2} \gamma_C \lambda_C^2 \lambda_D e^{-x/\lambda_D}. \tag{32}$$

Eq. 32 results from Eqs. 25 *a* and 26. It may be rewritten, using the definitions of γ_C and λ_C as

$$V_C = \frac{\rho_L I_0}{2} \frac{r_{BA}}{r_A} \lambda_D e^{-x/\lambda_D}. \tag{33}$$

Luminal voltage attenuation is described by

$$V_L = \frac{\rho_L I_0}{2} \left(\frac{m}{4} \lambda_E e^{-x/\lambda_E} + \lambda_D e^{-x/\lambda_D} \right). \tag{34}$$

Eq. 34 may be further simplified (from Eqs. 26 and 28) to

$$V_L = \frac{\rho_L I_0}{2} \lambda_D e^{-x/\lambda_D}. \tag{35}$$

Intraepithelial Injection of Current Along the lines discussed above, Eq. 24 *b* may be written as

$$V_L = \frac{\rho_C I_0}{2} \gamma_L \lambda_C^2 \lambda_D e^{-x/\lambda_D}, \tag{36}$$

and Eq. 24 *a* as

$$V_C = \frac{\rho_C I_0}{2} \left(\lambda_E e^{-x/\lambda_E} + \frac{m}{4} \lambda_D e^{-x/\lambda_D} \right). \tag{37}$$

Using the definitions of m, γ_L, γ_C, and λ_C, and recalling the approximation 30, Eqs. 36 and 37 are rewritten

$$V_L = \frac{\rho_L I_0}{2} \frac{r_{BA}}{r_A} \lambda_D e^{-x/\lambda_D}; \tag{38}$$

$$V_C = \frac{\rho_C I_0}{2} \lambda_C e^{-x/\lambda_C} + \frac{\rho_L I_0}{2} \left(\frac{r_{BA}}{r_A} \right)^2 \lambda_D e^{-x/\lambda_D}. \tag{39}$$

Eqs. 37 and 39 indicate that intraepithelial voltage attenuation is described by two (not one) exponential terms. To estimate the deviation from the single exponential to the biexponential decrement of voltage with distance (owing to electrical interactions), we computed through a simplified form of eq. 37 the value of V_C as a function of distance from the source (Fig. 2). To achieve this, we used appropriate values for λ_C, λ_D, and $m/4$, representative of the properties of the proximal tubule in *Necturus* (see below). Fig. 2 shows that although an experimental distinction between single and biexponential curves may prove quite difficult within 500 μm from the source, the paired ordinate points at abscissa 1,000 μm differ by a factor of two.

A REDEFINITION OF THE LENGTH CONSTANTS λ_D AND λ_C APPEARING IN THE ABOVE SIMPLIFIED EQUATIONS Inspection of Eqs. 35 and 36 shows that the length constant of the luminal cable is λ_D, whether the source is in the lumen or in the epithelium. This observation indicates that, if the assumptions 26 and 27 are correct, the luminal voltage attenuation curve, i.e., the single exponential term of slope λ_D, is not distorted by concomitant current and voltage spread along the epithelial cable. Within this framework, λ_D may be expressed as a function of the resistances of the tissue according to the relationship,[3]

$$\lambda_D = \left[\frac{r_{TE}}{\rho_L}\right]^{1/2} = \left[\frac{\alpha R_{TE}}{2\theta_L}\right]^{1/2}. \tag{40}$$

The epithelial length constant, λ_C, defined by the properties of the epithelial cable alone, is given by[3]

$$\lambda_C = \left[\frac{\beta(1 + \beta/2\alpha)}{\theta_C[G_A + G_B(1 + \beta/\alpha)]}\right]^{1/2}. \tag{41}$$

[3] Eq. 40 stems from Eq. 31, i.e.,

$$\frac{1}{\lambda_D^2} \simeq \frac{1}{\lambda_L^2}\left(1 - \frac{m}{4}\frac{\lambda_L^2}{\lambda_C^2}\right)$$

which, in combination with Eq. 17 yields

$$\frac{1}{\lambda_D^2} \simeq \frac{1}{\lambda_L^2}\left[1 - \frac{\gamma_L\gamma_C}{\left(\frac{1}{\lambda_C^2} - \frac{1}{\lambda_L^2}\right)^2}\frac{\lambda_L^2}{\lambda_C^2}\right]. \tag{4 F}$$

From inequality 1 F, the difference $(1/\lambda_C^2) - (1/\lambda_L^2)$ in approximation 4 F may be reduced to $(1/\lambda_C^2)$. Expressing then λ_L, λ_C, γ_L, and γ_C as a function of ρ_L, ρ_C, r_{BA}, r_{SA} and r_A (see their definitions), we obtain Eq. 40. Eq. 41 is developed from the definition of λ_C,

$$\lambda_C = \left[\frac{r_{BA}}{\rho_L}\right]^{\frac{1}{2}},$$

where

$$\frac{1}{r_{BA}} = \frac{1}{r_B} + \frac{1}{r_L} = \frac{2\pi\alpha}{R_L} + \frac{2\pi(\alpha + \beta)}{R_B} = 2\pi\alpha[G_L + G_B(1 + \beta/\alpha)], \tag{5 F}$$

Eq. 41 may be rewritten as

$$G_A + G_B\left(1 + \frac{\beta}{\alpha}\right) = \frac{\beta(1 + \beta/2\alpha)}{\lambda_C^2 \theta_C}. \tag{42}$$

AN EXPRESSION OF THE VOLTAGE ATTENUATION CURVES AS A FUNCTION OF SPECIFIC RESISTANCES AND RESISTIVITIES The general equations (Eqs. 24 *a*, 24 *b*, 25 *a*, 25 *b*), or better, their simplified forms (Eqs. 32–39) applicable to the proximal tubue of *Necturus*, may be written in a different form, in which V_L and V_C are expressed as a function of specific tissue conductances and conductivities:

Luminal Injection of Current

$$V_L = \frac{\theta_L I_0}{2\pi\alpha^2} \lambda_D e^{-x/\lambda_D}; \tag{43}$$

$$V_C = \frac{G_A}{G_B(1 + \beta/\alpha) + G_A} V_L. \tag{44}$$

V_L in Eq. 44 refers to Eq. 43.

Eq. 44 may be rewritten as

$$\frac{G_B}{G_A} = \left(\frac{V_L}{V_C} - 1\right) \frac{1}{1 + (\beta/\alpha)}. \tag{45}$$

Intraepithelial Injection of Current

$$V_L = \frac{\theta_L I_0}{2\pi\alpha^2} \frac{G_A}{G_B(1 + \beta/\alpha) + G_A} \lambda_D e^{-x/\lambda_D}; \tag{46}$$

$$V_C = \frac{\theta_C I_0}{4\pi\alpha\beta(1 + \beta/2\alpha)} \lambda_C e^{-x/\lambda_C} + \frac{G_A}{G_B(1 + \beta/\alpha) + G_A} V_L. \tag{47}$$

V_L in Eq. 47 refers to Eq. 46.

The Relationship Between Experimentally Determined Length Constants and the Actual Properties of the Proximal Tubule

The functions V_L and V_C defined above (general or simplified), describe the distribution of voltage along the entire length of the two concentric cables. In the experiments of this paper, the length constants of the luminal (λ_{LM}) and epithelial (λ_{CM}) cables were computed from two distinct measurements of V_L and/or V_C at abscissas x and x' (where $x' > x$), within a given range of distances from the source. The values of λ_{LM} and λ_{CM} are related to the

---

and

$$\rho_C = \frac{\theta_C}{\pi\beta(\beta + 2\alpha)} = \frac{\theta_C}{2\pi\alpha\beta(1 + \beta/2\alpha)}. \tag{6 F}$$

Combining Eqs. 5 *F* and 6 *F*, we obtain after rearrangement Eq. 41.

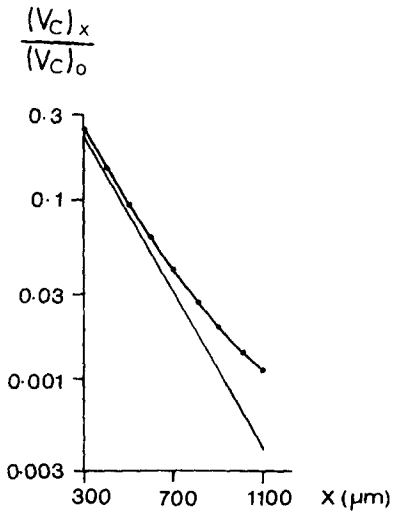

FIGURE 2. The dimensionless ratio $(V_C)_x/(V_C)_0$ (ordinate) was computed as a function of distance (abscissa) from an intraepithelial point source. The straight line describes a single exponential voltage attenuation curve, i.e., free from luminal interactions, of slope $\lambda_{CM_c} = \lambda_E = \lambda_C = 200$ μm. The upper curve (λ_{CM_c}) corresponds to a hypothetical cylindrical double cable, the main properties of which are: $\lambda_E = 200$ μm; $\lambda_D = 1{,}000$ μm; $(m/4)$ $(\lambda_D/\lambda_E) = 0.02$. They are similar to those of the proximal tubule of *Necturus* (see Results). Cable-to-cable interactions were taken into account in the construction of the theoretical voltage attenuation curve, in this case, by using Eq. 37. Eq. 37 may be also written (see approximation 30)

$$V_C = \frac{\rho_C I_0}{2} \lambda_C \left(e^{-x/\lambda_E} + \frac{m}{4} \frac{\lambda_D}{\lambda_E} e^{-x/\lambda_D} \right),$$

or

$$V_C/(\rho_C I_0 \lambda_C/2) = e^{-x/\lambda_E} \left(1 + \frac{m}{4} \frac{\lambda_D}{\lambda_E} e^x \left[1/\lambda_E - 1/\lambda_D \right] \right),$$

which is equivalent to

$$\log \left[V_C/(\rho_C I_0 \lambda_C/2) \right] = -\frac{x}{\lambda_E} + \log \left(1 + \frac{m}{4} \frac{\lambda_D}{\lambda_E} e^x \left[1/\lambda_E - 1/\lambda_D \right] \right).$$

The term $(\rho_C I_0 \lambda_C/2)$ provides an estimate of the potential at $x = 0$ (Eq. 37). Thus, we may plot in ordinate the dimensionless ratio $(V_C)_x/(V_C)_0$ and compute accordingly several abscissas at 100-μm intervals. It is clearly seen that the distortion produced by the luminal cable increases progressively with distance. So does the shift of λ_{CM_c} (curved line) away from λ_C (straight line). Actually, the value of an experimentally determined λ_{CM_c} varies as a function of the distance separating the recording microelectrodes from the source and from one another (see Fig. 12).

findings of the analytical treatment according to the following relationships:

$$\frac{1}{\lambda_{LM}} = \frac{\log V_{L(x')} - \log V_{L(x)}}{x - x'};$$

$$\frac{1}{\lambda_{CM}} = \frac{\log V_{C(x')} - \log V_{C(x)}}{x - x'}.$$

The above equations are general and apply to measurements performed in the lumen (V_L) and epithelium (V_C), respectively, irrespective of the source localization. Combined with Eqs. 18 *a* and 18 *b* they become

$$\frac{1}{\lambda_{LM}} = \frac{1}{x - x'} \log \frac{K_L e^{-x'/\lambda_E} + K_L' e^{-x'/\lambda_D}}{K_L e^{-x/\lambda_E} + K_L' e^{-x/\lambda_D}}; \tag{48}$$

$$\frac{1}{\lambda_{CM}} = \frac{1}{x - x'} \log \frac{K_C e^{-x'/\lambda_E} + K_C' e^{-x'/\lambda_D}}{K_C e^{-x/\lambda_E} + K_C' e^{-x/\lambda_D}}. \tag{49}$$

Eqs. 48 and 49 may be also rewritten as

$$\frac{1}{\lambda_{LM}} = \frac{1}{\lambda_D} - \frac{1}{x' - x} \log \frac{1 + \frac{K_L e^{-x'/\lambda_E}}{K_L' e^{x'/\lambda_D}}}{1 + \frac{K_L e^{-x/\lambda_E}}{K_L' e^{-x/\lambda_D}}}; \tag{50}$$

$$\frac{1}{\lambda_{CM}} = \frac{1}{\lambda_D} - \frac{1}{x' - x} \log \frac{1 + \frac{K_C e^{-x'/\lambda_E}}{K_C' e^{-x'/\lambda_D}}}{1 + \frac{K_C e^{-x/\lambda_E}}{K_C' e^{-x/\lambda_D}}}. \tag{51}$$

Another useful form of Eq. 51 is

$$\frac{1}{\lambda_{CM}} = \frac{1}{\lambda_E} - \frac{1}{x' - x} \log \frac{1 + \frac{K_C' e^{-x'/\lambda_D}}{K_C e^{-x'/\lambda_E}}}{1 + \frac{K_C' e^{-x/\lambda_D}}{K_C e^{-x/\lambda_E}}}. \tag{52}$$

Eqs. 50–52 are used in Footnotes 3 and 4 to warrant the validity of assumptions 26 and 27 and resulting simplifications, a posteriori, i.e., by taking into account pertinent experimental observations.

METHODS

General

All experiments were carried out at room temperature on the in vivo *Necturus* kidney. Details for anesthesia and preparation of the animals have been already described

(6). Similarly, the procedure for filling microelectrodes and the methodology for electrical measurements have been given elsewhere (1–3). The recording was achieved with one or two electrometers (Keithley Instr., Inc., Cleveland, Ohio, model 604 and/or Medistor, model A-35, W. H. Associates, Seattle, Wash.) connected to a multiway linear pen recorder (Watanabe Instrument Co., Tokyo, Japan, type WTR 281 or Linear Instr. Corp., Irvine, Calif., model 395). Injection of current was accomplished (*a*) by a voltage stimulator (Electromed, Paris, France—voltage range 0–200 V) through a 1,000 MΩ series resistor or (*b*) via a voltage source in series with a 100 MΩ resistor, the current passing through the microelectrode being made independent of electrode resistance by means of an operational amplifier feedback system. Current was delivered as rectangular waves lasting 1 s every 4 or 5 s. Current intensity was usually 100 nA.

Experimental Protocols

Seven groups of experiments were performed. They are described below.

GROUP I: DETERMINATION OF THE VOLTAGE ATTENUATION CURVE AFTER LUMINAL INJECTION OF CURRENT One or two microelectrodes were used, in addition to the current injecting tip. Their luminal position was ascertained from the shift in potential difference (PD) observed when they crossed the luminal membrane, from cell to lumen. It was subsequently warranted by measuring the magnitude of the electrotonic potential at the recording site. If either of the tips was out of the lumen (surface of the kidney or interstitium) we observed no significant coupling; i.e., the shift in PD was < 0.5 mV at the recording site. Correct localization of all the tips at the same time resulted in appreciably larger changes, on the order of 2–10 mV (e.g., see Figs. 3 and 7). Since the advancement of a recording microelectrode could displace the source electrode, current injection was on occasion interrupted to check the position of the source, by switching it reversibly from the current generator to a recording device. When a single recording microelectrode was used, it was inserted in succession at two different sites in single tubules, the point source remaining unmoved. Interelectrode distance was measured with a micrometer eyepiece. The amplitude of the transepithelial electrotonic potential, $(V_L)_x$ and $(V_L)_{x'}$ corresponding to the abscissas x and x' of each tubule, was plotted on a semilog scale as a function of distance. Thus, the length constant λ_{LM_l} could be assessed individually for each tubule.

GROUP II: DETERMINATION OF THE INTRAEPITHELIAL VOLTAGE ATTENUATION CURVE AFTER INTRACELLULAR INJECTION OF CURRENT IN FREE-FLOW TUBULES Three microelectrodes were inserted into the epithelial layer of single tubules, one for injection of current and two for recording. The intracellular position of the tips was easily ascertained from the recorded intracellular negativity; the position of the source was repeatedly checked subsequently by the method described above. We determined the apparent length constant of each tubule, λ_{CM_c} separately.

GROUP III: INTRAEPITHELIAL VOLTAGE ATTENUATION, AFTER INTRACELLULAR INJECTION OF CURRENT IN OIL-FILLED TUBULES The procedure described above was applied in tubules previously filled with oil. Under these circumstances, current flow from cell interior to interstitium through the series resistances of luminal membrane and shunt pathway, i.e., the limb R_Z, was essentially suppressed. Current could leave the cellular layer only across the basolateral membrane. It may be argued that despite luminal introduction of oil, a thin layer of conducting fluid sticks to the brush border around the oil column. However, the thickness of that layer presumably does not exceed 1 μm; i.e., its cross-sectional area represents only a minute fraction of the total cross-sectional luminal surface. Thus, the residual longitudinal luminal conductance (physiologically connecting R_L to R_S and being proportional to cross-sectional area) may be considered negligible when the lumen is filled with oil.

GROUP IV: DETERMINATION OF A RATIO OF RESISTANCES FROM A RATIO OF VOLTAGES Under certain circumstances, to be defined in Results, the injection of current into the lumen of the tubule via a point source and the measurement of the ratio of voltages V_L/V_C at an abscissa x, at some distance from the source, allows an estimate of the ratio of cell membrane resistances:

$$V_L/V_C = 1 + (r_A/r_B). \tag{53}$$

It should be stressed that the above ratio of voltages measures a ratio of resistances per unit length, not the ratio of specific membrane resistances; taking into account the geometry of the tubule, it can be easily shown that the ratio r_A/r_B is equivalent to $r_A[1 + (\beta/\alpha)]/R_B$, not to R_A/R_B (as stated above, R_B refers to the "apparent" outside surface of the tubule, the area of the lateral membranes is not taken into account). The experiments were performed by introducing the current injecting microelectrode into the lumen and a single recording tip, stepwise, through the first cellular layer into the lumen and then into the second layer. Care was taken to make this impalement perpendicular or so to the tubular axis, so as to record V_C at both cellular layers in addition to V_L, all of them at a single abscissa. The intraluminal position of the source was checked on occasion by the procedure already described. The V_L/V_C ratio, obtained from this series of experiments, was plotted as a function of distance from the source.

GROUP V: DETERMINATION OF THE RATIO OF VOLTAGE DROPS ACROSS THE LUMINAL MEMBRANE AND THE WHOLE EPITHELIUM, AFTER INTRACELLULAR INJECTION OF CURRENT Basically the experimental protocol was similar to the previous one, with the exception of the positioning of the point source electrode which was introduced into the cellular layer. V_C (at both layers) and V_L were determined as above. The ratio $(V_C - V_L)/V_C$ was plotted as a function of the distance from the source.

GROUP VI: INTRALUMINAL INJECTION OF CURRENT AND PAIRED MEASUREMENTS (LUMINAL AND EPITHELIAL) OF THE ELECTROTONIC POTENTIAL AT TWO ABSCISSAS, x AND x' The current injecting microelectrode was inserted at once into the lumen. Then, two recording microelectrodes were advanced simultaneously and carried stepwise into (*a*) the superficial cell layer, (*b*) the lumen, and (*c*) the deeper epithelial layer. Their direction was roughly perpendicular to the tubular axis, in order to keep constant the distance of each microelectrode from the source, throughout the impalement. Thus paired V_C and V_L measurements were obtained at both abscissas x and x'. The position of the point-source electrode was frequently checked by switching it from the current generator to an electrometer. Successful experiments were defined by a constant position of the luminal source associated with the recording of V_C (at at least one epithelial layer) and V_L, both at abscissas x and x'.

GROUP VIII: INTRAEPITHELIAL INJECTION OF CURRENT ASSOCIATED WITH PAIRED MEASUREMENTS (LUMINAL AND EPITHELIAL) OF THE ELECTROTONIC POTENTIAL AT TWO ABSCISSAS x AND x' The procedure for recording was similar to that described above. The point-source electrode was inserted into the epithelial layer; it was often switched back and forth from the current generator to an electrometer, to ascertain its intracellular position. In this way the recorded paired values of V_C and V_L could be safely ascribed to current spread originating in an intracellular point source.

An Evaluation of the Conductive Properties of the Tissue According to Traditional Techniques

For the sake of comparison the transepithelial resistance, the resistances of cell membranes and that of the shunt pathway as well as the core resistivity of the epithelial cable were also computed separately, using the traditional equations, in which interactions between luminal and epithelial cables are not taken into account.

Within this framework r_{TE} and R_{TE} are usually expressed as a function of λ_{LM_l}:

$$\lambda_{LM_l} = \left[\frac{\alpha R_{TE}}{2\theta_L}\right]^{1/2} = \left[\frac{r_{TE}}{\rho_L}\right]^{1/2}. \tag{54}$$

Eq. 54 is identical to Eq. 40. Assuming the specific resistivity of the lumen, θ_L, to be 100 Ω·cm, i.e., the figure of biological fluids of amphibia and artificial solutions having the composition of the proximal tubular fluid in *Necturus*, the core resistivity per unit length, ρ_L, is given (21) by

$$\rho_L = 2V_{TE}/I_0\lambda_{LM_l}e^{-x/\lambda_{LM_l}}, \tag{55}$$

from which the "electrical" radius (α) of the tubule may be computed:

$$\alpha = [\theta_L/\pi\rho_L]^{1/2}. \tag{56}$$

In the intraepithelial cable, the monoexponential portion of the voltage attenuation curve is described (3, 4) by

$$V_C = \frac{I_0}{4\pi\alpha}\left[\frac{\theta_C}{G_{PAR}\beta}\right]^{1/2} e^{-x/\lambda_{CM_c}}, \tag{57}$$

where the length constant λ_{CM_c} is defined by

$$\lambda_{CM_c} = \left[\frac{\beta}{\theta_C G_{PAR}}\right]^{1/2}. \tag{58}$$

Combination of Eqs. 57 and 58 yields θ_C:

$$\theta_C = 4\pi\alpha\beta V_C/I_0\lambda_{CM_c}e^{-x/\lambda_{LM_c}}. \tag{59}$$

What is usually done, is to compute θ_C from Eq. 59 and insert its value into Eq. 58 to obtain G_{PAR}. However, one of the assumptions used to develop Eqs. 57 and 59 was that the lumen is infinitely conductive (4). This assumption is a rough approximation and, consequently, so is the calculated sum of cell membrane resistances (R_{PAR}) in free-flow tubules. By contrast in oil-filled tubules, leaks of current across the limb R_Z are suppressed because $R_Z \rightarrow \infty$. Thus, any error that could be introduced by the assumption of an infinitely conductive luminal fluid, in the calculation of G_{PAR}, is eliminated by luminal injection of oil. Thus, Eqs. 57–59 are adequate to compute peritubular membrane conductance alone, in oil-filled tubules; G_{PAR} should be then replaced by G_B.

RESULTS

Determination of the Luminal Length Constant λ_{LM_l} (Group I)

Fig. 3 depicts voltage attenuation along the lumen of the proximal tubule as a function of distance from the source. Straight lines indicate the slopes of the log V_L vs. x plot in 14 tubules. The measurements of V_L were performed either with two separate recording tips, in addition to the point-source (○) or with a single recording microelectrode inserted in succession at two different abscissas (●). The average length constant (λ_{LM_l}) of the first group of

experiments (three intraluminal microelectrodes) was 1,140 ± 246 μm, $n = 6$, when in the second group λ_{LM_l} was 950 ± 57 μm, $n = 8$. Since the difference between these means was not statistically significant ($P > 0.3$), the data were pooled to yield a single average length constant λ_{LM_l} of 1,031 ± 108 μm (range 520–1900 μm).

A comparison of our experimental observations with the analysis undertaken in the Theoretical Considerations section allows some simplification of the equations describing luminal voltage attenuation. As a result, the transepithelial resistance of the proximal tubule in *Necturus* kidney may be assessed from the measured length constant λ_{LM_l}, using ordinary cable equations (compare Eqs. 40 and 54)); i.e., there is no appreciable distortion of λ_{LM_l} from concomitant current spread along the epithelial cable. To estimate r_{TE} and R_{TE}, we computed the core resistivity per unit length, ρ_L, for each tube separately, according to Eq. 55; the average value of ρ_L was (142.2 ± 22) × 10^4 Ω/cm. From the individual figures of ρ_L the luminal radii were calculated, according

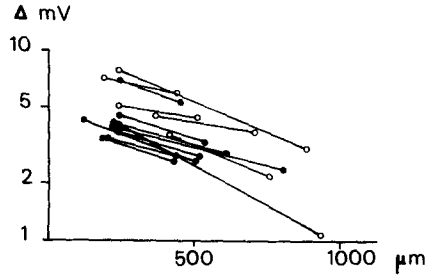

FIGURE 3. Voltage attenuation along the luminal cable. The current-injecting microelectrode was in the lumen. Two additional tips (○) or one microelectrode inserted in succession at two different sites (●) were used for recording.

to the Eq. 56. The average radius, α, was 52.5 ± 3 μm (range 31–73 μm), a value in close agreement with optical measurements reported by others (5, 7). Last, the specific transepithelial resistance R_{TE} could be assessed at 422 ± 68 Ω·cm^2 and the resistance per unit length r_{TE} at (1.26 ± 0.15) × 10^4 Ω·cm (Eqs. 40 and 54).

The observation of an "electrical" radius essentially identical to the optical luminal radius strongly suggests that the main resistive barrier to transepithelial current flow is at or very near the apical barrier of the cells. Otherwise, if the luminal and epithelial cables were an electrical syncitium, limited by the basolateral membrane, the electrical radius would have been closer to the sum ($\alpha + \beta$) rather than to the radius α.

Determination of the Intraepithelial Length Constant λ_{CM_c} in Free-Flow Tubules (Group II)

The data on voltage attenuation along the epithelial cable are plotted in Fig. 4. They are divided into two groups. The first group includes all determinations in which the distance between the source and the closest V_C reading was smaller than 300 μm (●). In the second group, the closest electrical measure-

ment was performed at a distance of 300 μm or beyond 300 μm from the source (○). As anticipated, the length λ_{CM_c} was slightly smaller in the first group, because of the distortion observed near the source in cables with bidimensional current spread (4, 17, 25): 214 ± 29 μm, $n = 5$; against 253 ± 21 μm, $n = 13$, range 152–400 in the second group. Although the difference was not statistically significant ($P > 0.3$), the distinction is outlined because only the data of the second group are likely to reflect the portion of the voltage attenuation curve not distorted by bidimensional spread of current near the source (3, 4).

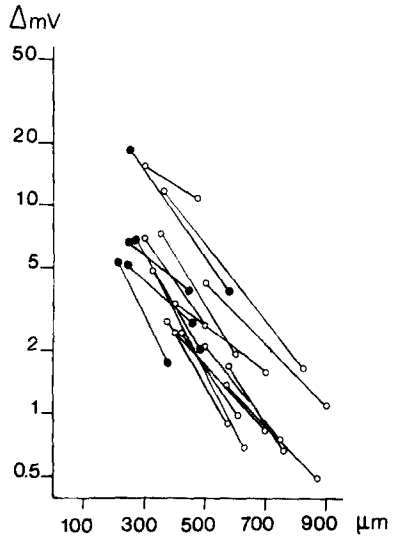

FIGURE 4. Voltage attenuation along the epithelial cable (free-flow experiments). Single tubules were studied with three intracellular microelectrodes (source and two recording tips). The data are divided into two groups, based on the distance separating the source from the closest to its record tip. (●) This distance was smaller than 300 μm; (○) distances were equal to or greater than 300 μm.

Traditionally the slope of voltage attenuation of the epithelial cable, λ_{CM_c}, is used to compute the sum of cell membrane resistances in parallel. This is based on the wrong assumption of no electrical interactions between luminal and epithelial cables in *Necturus* kidney. Eqs. 39 and 47 show that the voltage attenuation curve of the epithelial cable is the sum of two exponential terms; their respective slopes cannot be assessed by the determination of V_C only at two abscissas per tubule. Thus, the data of this series provide only a basis for comparison with other studies: the apparent (measured) length constant of the epithelial cable has been reported to be 200 μm in the in vivo (29) and in the perfused *Necturus* kidney (4), a figure in good agreement with our average λ_{CM_c} of 253 μm. It will be shown later that λ_{CM_c} may vary with distance from the source. For this reason it lacks physiological meaning.

Determination of the Intraepithelial Length Constant λ_{CM_c} in Tubules Filled with Oil (Group III)

The results of such experiments are schematically shown in Fig. 5. The symbols are as in Fig. 4. In the experiments in which the measurements were performed at or beyond 300 μm from the source, the average length constant was 179 ± 18 μm (n = 9, range 107–285). The average λ_{CM_c} of 155 ± 9 μm (n = 11) observed in tubules in which one electrical determination was within 300 μm from the source is only mentioned for comparison, not used subsequently. The two means differ significantly on a statistical basis ($P < 0.03$). From Eq. 59, in which β was taken as 25 μm (5) and α as 52.5 μm, the average specific core conductivity θ_C could be estimated at 5,436 ± 1,925 Ω·cm (n =

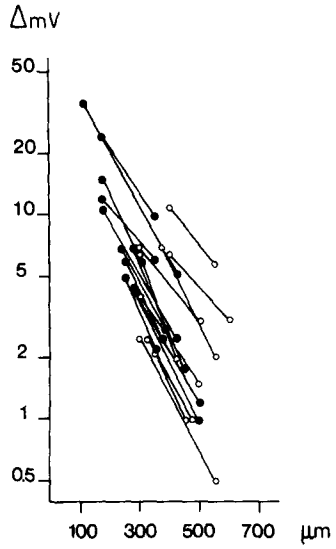

FIGURE 5. Voltage attenuation along the epithelial cable in oil-filled tubules. Three intracellular microelectrodes were used. Symbols as in Fig. 4.

9, range 1,503–17,118) and the value of R_B (Eq. 58) at 508 ± 104 Ω·cm^2 (range 181–989). Since by definition $r_B = R_B/2\pi(\alpha + \beta)$, the average r_B is 1.04×10^4 Ω·cm.

The Determination of the Ratio of Voltages V_L/V_C, as a Function of Distance from a Luminal Source (Group IV)

When current is passed from lumen to interstitium across an epithelium and, by means of an intracellular microelectrode, the ratio of voltages V_L/V_C is measured, the ratio r_A/r_B (Eq. 53) may be estimated from V_L/V_C provided that transepithelial current density is uniform. In renal tubules, studied by the technique of a luminal point source, transepithelial current density is not uniform. However, if the current flowing out of the lumen along the transcellular route, per unit of tubular length, is a constant fraction of the current left in the lumen at each abscissa, then, the V_L/V_C ratio is independent of

interelectrode distance. An additional requirement to satisfy this condition (the constancy of V_L/V_C) is that no longitudinal current spread occurs along the epithelium. Thus, the constancy of the V_L/V_C ratio (if observed) would imply that V_C arises solely as a result of transcellular flow of current out of the lumen, not from intraepithelial current spread downstream consecutive to an intracellular source, "actual" or "equivalent." If the latter were to occur (i.e., intraepithelial current spread from cell to cell), the V_L/V_C ratio could not remain constant along the x axis.

Fig. 6 shows that the value of $(V_L/V_C) - 1$ is indeed independent of interelectrode distance. The calculated regression line of $Y = 0.00X + 2.79$ is parallel to the abscissa; i.e., the drop of voltages across luminal and basolateral membranes is in a fixed ratio over a wide range of distances from the source. Under these circumstances, the average value of $(V_L/V_C) - 1 = 2.8 \pm 0.45$, $n = 39$, does measure the ratio of cell membrane resistances r_A/r_B (Eq. 53). Recalling that $r_B = 1.04 \times 10^4\ \Omega\cdot$cm, r_A may be estimated at $2.91 \times 10^4\ \Omega\cdot$cm and r_{TC} at $3.95 \times 10^4\ \Omega\cdot$cm. From r_{TE}, measured above, and the present figure of r_{TC}, r_S may be computed at $1.85 \times 10^4\ \Omega\cdot$cm; thus $r_{TC}/r_S = 2.14$. Since $r_A = R_A/2\pi\alpha$ and $r_S = R_S/2\pi\alpha$, the corresponding specific resistances are $R_A = 960\ \Omega\cdot\text{cm}^2$ and $R_S = 610\ \Omega\cdot\text{cm}^2$. From the value of $R_B = 508$

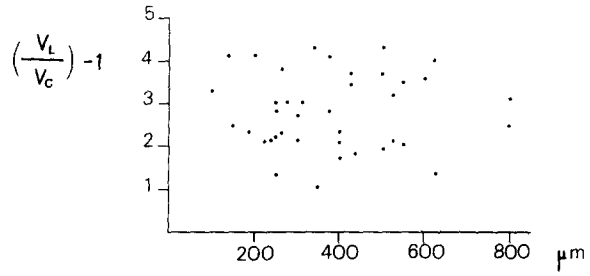

FIGURE 6. The magnitude of the difference $(V_L/V_C) - 1$ is expressed as a function of distance from the luminal point source.

$\Omega\cdot\text{cm}^2$, the transcellular specific resistance R_{TC} is 1468 $\Omega\cdot\text{cm}^2$ and the ratio $R_{TC}/R_S = 2.4$. One of the recordings used to assess V_L and V_C at a single abscissa is reproduced in Fig. 7.

The Determination of the Ratio of Voltages V_L/V_C as a Function of Distance from an Intraepithelial Source (Group V)

The argument developed above as to the identity of $(V_L/V_C) - 1$ and r_A/r_B could be hardly extended to compute independently the r_L/r_S ratio from paired measurements of V_L and V_C at different abscissas, using an intracellular point source. Indeed upon intraepithelial injection of current, r_L/r_S would be equal to $(V_C - V_L)/V_L$ only if all intraepithelial current were to leave the cell layer solely across the R_Z limb ($r_B \simeq \infty$), i.e., if the $(V_C - V_L)/V_L$ ratio were constant. Fig. 8 shows that this ratio decreases sharply as interelectrode distance increases. It bears a negative sign at long distances from the source, i.e., when V_C becomes smaller than V_L (this indeed occurs, see e.g., Fig. 11). Obviously, the r_L/r_S ratio cannot be computed from these experiments.

Another complication may arise with this technique when the recording tip is quite close to the source, i.e., at abscissas at which circumferential current density is not yet uniform. Then, the value of the intracellular electrotonic potential V_C differs greatly from one cellular layer to another, as illustrated in Fig. 9.

Intraluminal and Intraepithelial Voltage Attenuation after Luminal Injection of Current (Group VI)

In this series of experiments voltage attenuation was assessed at both epithelial and luminal cables, after luminal injection of current. Paired measurements

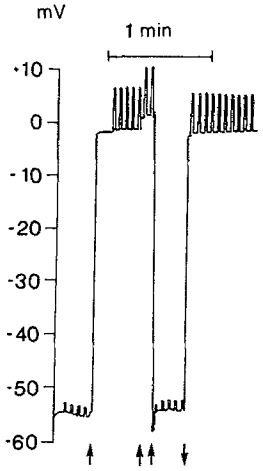

FIGURE 7. This is a recording reproduced from an experiment designed to measure the voltages recorded across the peritubular membrane and transepithelially at the same abscissa x. The current-injecting microelectrode is in the lumen. The recording tip is at once into the superficial cell layer. It records cell membrane PD and, on top of it, the electrotonic potential V_C (the vertical pulses superimposed upon the base-line PD). V_C arises as a result of current flow out of the lumen along the transcellular route, at the recording site. Advancement of the tip into the lumen (first arrow) allows an assessment of the transepithelial PD and of the transepithelial electrotonic potential V_L (the larger pulses associated with the transepithelial PD). At the second arrow, a new advancement of the tip brings about a small change in transepithelial base-line PD, probably related to a change of tip resistance. There is no change in transepithelial input conductance (V_L remains unaltered). Further advancement of the tip (third arrow) brings it into the opposite, deep cellular layer). At last it is withdrawn into the lumen (fourth arrow, downwards).

were performed in single tubules; V_C and V_L were determined, each of them at two identical abscissas, by means of two separate microelectrodes. The results are schematically represented in Fig. 10. The paired $\lambda_{CM_l}/\lambda_{LM_l}$ ratios in single tubules were 820/425, 790/1,160, 1,600/2,000, 730/1,400, 1,550/750, 1,080/950 and 950/580, yielding an average $\lambda_{CM_l}/\lambda_{LM_l}$ of 1.02 ± 0.21.[4] The

[4] The experiments of group VI indicate that, upon luminal injection of current, the paired luminal and epithelial length constants obtained in single tubules are equal to one another; i.e.,

mean length constant of the luminal cable λ_{LM_l} amounts to 1,074 ± 136 μm, a figure comparable to the average of 1,031 μm reported above ($P > 0.5$). The average length constant of the epithelial cable λ_{CM_l} = 1,038 ± 203 μm is very close to that of its companion luminal cable λ_{LM_l} ($P > 0.5$), and to the λ_{LM_l} of 1,031 μm already mentioned ($P > 0.9$). Thus, upon luminal injection

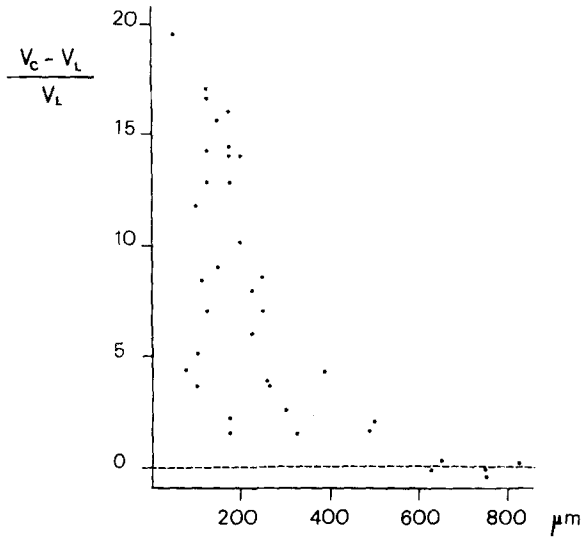

FIGURE 8. The magnitude of the ratio $(V_C - V_L)/V_L$ is expressed as a function of distance from an intracellular point source. Note that beyond 600 μm, the apparent $(V_C - V_L)/V_L$ ratio becomes on occasion negative.

of current a major shift of the length constant of the cell cable occurs. The epithelial length constant λ_{CM_l} becomes then at least four times greater than the epithelial length constant λ_{CM_c} obtained with cellular injection of current

---

$\lambda_{LM_l} = \lambda_{CM_l} \cdot \lambda_{LM_l}$ and λ_{CM_l} were determined by measuring the electrotonic potential V_L at two abscissas x and x', and V_C at the same abscissas. Thus, λ_{LM_l} and λ_{CM_l} are literally defined by Eqs. 50 and 51. Since $\lambda_{LM_l} = \lambda_{CM_l}$, these expressions are equal to one another. As a result, the logarithmic expression appearing in Eq. 50 is equal to that of eq. 51. By taking into account the values of K_L, K'_L, K_C, and K'_C (they are given by Eqs. 23 *a*, 23 *b*, and 23 *c*, since in the experiments of group VI the source was in the lumen), it is easily demonstrated that the equality of the two logarithms of Eqs. 50 and 51 cannot be fulfilled unless $\lambda_E e^{-x/\lambda_E} \ll \lambda_D e^{-x/\lambda_D}$. Thus, the experimental data warrant so far one of the two assumptions [inequality 26] used in the theoretical section to simplify the general equations describing voltage attenuation in cylindrical concentric cables, when applied to the proximal tubule of *Necturus*. Incidentally, it may be also noticed that the above measured length constants ($\lambda_{LM_l} = \lambda_{CM_l}$) provide an estimate of λ_D. Indeed, upon luminal injection of current, the logarithmic expression of Eqs. 50 and 51 becomes negligibly small (we use again the definitions of K_L, K'_L, K_C, and K'_C as above in association with inequality 26) and may be omitted. Thus, Eqs. 50 and 51 simplify to

$$\lambda_D = \lambda_{LM_l} = \lambda_{CM_l}. \qquad (7\,F)$$

λ_{LM_l} and λ_{CM_l} refer to experimental determinations (luminal source), when λ_D refers to the properties of the proximal tubule irrespective of the technique used to assess them.

(200–250 μm); interestingly, not only λ_{CM_l} is significantly greater than λ_{CM_c} but, more importantly, it falls into line with λ_{LM_l}. Obviously the spread of current and voltage along the lumen of the tubule distorts the pattern of voltage attenuation in the companion epithelial cable. More generally, we may infer that when the luminal electrotonic potential $(V_L)_x$ is larger than

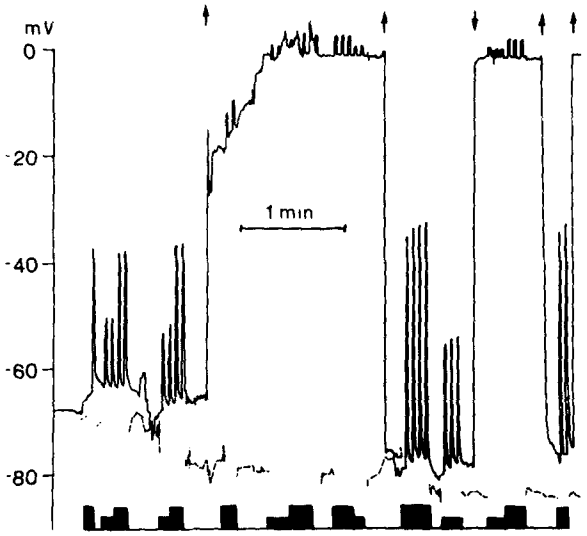

FIGURE 9. Reproduction of a recording from an experiment designed to study the ratio $(V_C - V_L)/V_L$ (plotted as a function of distance in Fig. 8). The source was in a cell of the deeper layer. Its intracellular position was ascertained by shifting the microelectrode back and forth from the current-injecting device to an electrometer. The PD at the source is indicated by the dotted line. Injection of current is schematically represented by the horizontal bars at the bottom of the figure: single height 100 nA; double height 200 nA. At the start of the figure, the recording tip is in a cell of the superficial layer. Note that the injection of 100 nA produces about 13–15 mV shift in PD (V_C is given by the pulses superimposed upon membrane PD), when injection of 200 nA gives rise to an electrotonic potential (V_C) of 26–29 mV. At the first arrow, the microelectrode is advanced. The result is a loss of PD. The recorded potential of about −20 mV is anything but stable. It slowly drifts towards and stabilizes at a plateau of −1 to −2 mV. The magnitude of V_L during the drift is barely higher than that obtained when the transepithelial PD has stabilized. Thus, the apparent transepithelial PD of about −20 mV (slowly decreasing subsequently) corresponds to residual intracellular potential, after an incomplete passage of the tip into the lumen. That the tip was readily into the lumen upon recording of −1 to −2 mV is confirmed by further advancement of the microelectrode into the second cellular layer (second arrow). Here, injection of current via the source microelectrode gives rise to V_C values higher than those observed in the superficial layer: 24 mV (100 nA) and 44 mV (200 nA). Withdrawal of the recording tip into the lumen (single downward arrow) and reentering into the deep layer (next upward arrow) shows that the effects of current injection (V_L and V_C) are largely reproducible. At last the tip is advanced into the interstitium (last arrow).

the corresponding intraepithelial electrotonic potential $(V_C)_x$ in *Necturus* kidney, the luminal pattern of voltage attenuation will be reproduced by the epithelial cable, irrespective of source localization.

Intraepithelial and Intraluminal Voltage Attenuation after Intracellular Injection of Current (Group VII)

Fig. 11 shows schematically the pattern of voltage attenuation in epithelial and luminal cables, consequent to intraepithelial injection of current. The values of the five paired length constants (cellular/luminal) of Fig. 11 were 210/865, 210/1,060, 175/1,160, 250/840, and 180/1,300. The mean of the

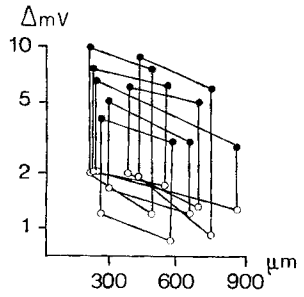

FIGURE 10. Intraluminal injection of current and paired measurements of voltage attenuation along the luminal and epithelial cables. Two recording microelectrodes were used in each experiment to study V_C (○) and V_L (●) at their respective abscissas. The resulting four determinations are connected by straight lines to form a quadrilateral; a vertical line is used for each abscissa. In each experiment, the two higher readings correspond to V_L, the lower ones to V_C.

intraepithelial slopes was 205 ± 13 μm, a figure not too different from the above reported λ_{CM_c} of 253 μm in another series of free flow experiments ($P > 0.1$). More importantly, the average length constant of the corresponding luminal cables λ_{LM_c} (1,045 ± 87 μm) was significantly different from that of their companion cell cables ($P < 0.001$), but identical to the λ_{LM_l} of 1,031 μm obtained after luminal injection of current ($P > 0.9$).[5] This set of experiments, taken together with the data of group VI underscores the independence of the pattern of luminal voltage attenuation with respect to source localization. The measured λ_{LM_c} (present series) of 1,045 μm and the value of λ_{LM_l} of 1,031 and

[5] In this footnote we produce evidence supporting assumption 27. Since we have established that $\lambda_E e^{-x/\lambda_E} \ll \lambda_D e^{-x/\lambda_D}$, (footnote 3) the logarithmic expression appearing in Eq. 52 is a finite and positive quantity which cannot be neglected. Eq. 52 states that $1/\lambda_{CM}$ is the difference of two positive terms, the greater of which is $1/\lambda_E$. Thus $1/\lambda_E > 1/\lambda_{CM}$; i.e.,

$$\lambda_{CM} > \lambda_E. \qquad (8\,F)$$

Note that since Eq. 52 is a general expression of λ_{CM}, independent of source localization, the inequality 8 F applies to all situations, including those in which the source was intraepithelial; i.e., $\lambda_{CM_c} > \lambda_E$. Recalling that $\lambda_{LM_l} = \lambda_{LM_c}$ (VI and VII set of experiments) and $\lambda_{LM_l} = \lambda_D$ (Eq. 7 *F*), we may write

$$\lambda_{LM_c} = \lambda_D. \qquad (9\,F)$$

1,074 (luminal injection of current, groups I and VI) are for all practical purposes identical. Clearly, intraepithelial injection of current gives rise to voltage spread into the lumen, similar to that obtained with a luminal source.

We interpret this finding as follows: upon intraepithelial injection of current, a large fraction of the injected current flows from cell to lumen near the source. This current remains essentially inside the lumen; it gives rise to voltage attenuation along the luminal cable undistorted from epithelial interactions because (*a*) V_C decays quickly and becomes within a few hundred micrometers similar to or smaller than V_L [the ratio V_C/V_L in Fig. 11 is on the

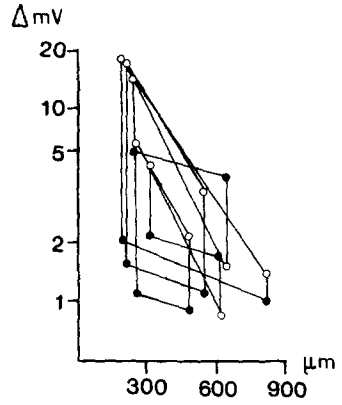

FIGURE 11. Paired measurements of voltage attenuation in epithelial and luminal cables, after intraepithelial injection of current. Two recording microelectrodes were used to measure V_C (○) and V_L (●) at two different abscissas. Each experiment is represented by four points connected by straight lines. Vertical lines indicate the common abscissa of single microelectrodes. In all studied tubules, V_C was always greater than the homologous V_L at the closest to the source abscissa. By contrast, V_C became smaller than the corresponding V_L in two experiments at the most remote abscissa.

average 6.0 ± 1.70 at 200–300 μm from the source (abscissa x) against 1.6 ± 0.6 at 500–800 μm (abscissa x')] and (*b*) even within this initial portion of the tubule, current flows from cell to interstitium preferentially across the basolateral resistance rather than through the limb R_Z ($R_B < R_Z$). Conceivably, at larger distances from the source, e.g., beyond 1,000 μm, V_C is much smaller than V_L and the luminal electrotonic potential interferes with V_C, altering accordingly, λ_{CM_c}, even though the source is epithelial. λ_{CM_c} flattens progressively becoming eventually identical to λ_{LM_c}. In two tubules in which the closest to the source abscissa, x, was 700 μm (current intensity was 200 nA to

---

Dividing inequality 8 *F* by Eq. 9 *F* we obtain $\lambda_{CM_c}/\lambda_{LM_c} > \lambda_E/\lambda_D$ and a fortiori $\lambda^2_{CM_c}/\lambda^2_{LM_c} > \lambda^2_E/\lambda^2_D$. Since it was established (VII set of experiments) that $\lambda^2_{CM_c}/\lambda^2_{LM_c} \simeq 0.05$, i.e., $\lambda^2_{CM_c}/\lambda^2_{LM_c} \ll 1$, we infer a fortiori that $\lambda^2_E/\lambda^2_D \ll 1$. Thus, the second assumption (inequality 27) used to simplify the general equations (Eqs. 24 *a*, 24 *b*, 25 *a*, and 25 *b*) to the particular case of the proximal tubule of *Necturus* is warranted by the experimental findings of this paper.

provide detectable V_C readings at x'), the measured slopes λ_{CM_c} were 400 and 450 μm (not included in the data of Figs. 4 and 11). They are larger than the mean λ_{CM_c} of some 200–250 μm reported above. These observations are consistent with the notion that the slope of intraepithelial voltage attenuation in free-flow should not be used to estimte R_{PAR} as previously done.

Indeed, contrary to λ_{LM_c} and λ_{LM_l} (the luminal voltage attenuation slopes), which are approximately equal to λ_D ($\lambda_{LM_c} \simeq \lambda_{LM_l} \simeq \lambda_D$), there is no simple relationship between λ_{CM_c} and λ_C, λ_E, or λ_D (Eq. 39 and Fig. 2). We have computed, on the basis of the theoretical findings of Fig. 2, the magnitude of λ_{CM_c} as a function of the location of the three microelectrodes (source and two recording tips) in relation to one another (Fig. 12). It is clearly seen that λ_{CM_c} does vary even when all measurements are performed within 1,000 μm from the source. This observation largely accounts for the observed differences in λ_{CM_c} between groups II and VII of this study.

An Estimate of the Conductive Properties of the Proximal Tubule According to the Analysis Undertaken in the Theoretical Considerations Section

We shall attempt hereafter an estimate of the conductive properties of the proximal tubule, by taking into account electrical interactions arising between the luminal and epithelial cables. To do so, paired determinations of V_L and V_C at two abscissas (groups VI and VII) will be used and inserted into appropriate equations of the theoretical section.

From the data of group VII, the term $(G_A)/G_B(1 + \beta/\alpha) + G_A = F_1$ may be computed separately for each tubule according to Eq. 46. V_L is measured, $\theta_L = 100\ \Omega\cdot$cm, α is taken as 52.5×10^{-4} cm, $I_0 = 10^{-7}A$, and λ_D was shown to be equal to λ_{LM_c} (Eq. 9 *F*). The value of F_1 was on the average 0.52 ± 0.12 ($n = 5$). Then, Eq. 47 is used in its logarithmic form, as

$$\log[(V_C)_x - F_1(V_L)_x] - \log \frac{\theta_C I_0 \lambda_C}{4\pi\alpha\beta(1 + \beta/2\alpha)} = -\frac{x}{\lambda_C} \qquad (47b)$$

to compute λ_C. Since Eq. 47 *b* contains two unknowns, λ_C and the logarithm of the ratio $(\theta_C I_0 \lambda_C)/4\pi\alpha\beta(1 + \beta/2\alpha) = F_2$, paired measurements of V_C and V_L, at two abscissas x and x' in each tubule, are necessary to obtain the value of λ_C and F_2, via a system of two equations and two unknowns. The data of group VII were used again. The five λ_C (not λ_{CM_c}) figures, thus computed were 210, 225, 205, 205, and 105 μm, and their average was 190 ± 48 μm. Discarding the last figure of this group (105 μm), which was only half as much as the four other values, the mean λ_C becomes 211 ± 9 μm.

The above system of two unknowns and two equations yields also an estimate of F_2. Recalling that $F_2 = (\theta_C I_0 \lambda_C)/4\pi\alpha\beta(1 + \beta/2\alpha)$, the value of θ_C may be now assessed. It was 2,894, 2,325, 1,414, 2,754, and 9,952. Discarding the last tubule, as above, we obtain an average θ_C of $2{,}347 \pm 333\ \Omega\cdot$cm.

The experiments of the group VI provide a means to estimate the ratio V_L/V_C at 3.85 ± 0.34. From Eq. 53 we obtain $(V_L/V_C) - 1 = r_A/r_B = 2.85$. Converting r_A/r_B to R_A/R_B ($= G_B/G_A$) we have $G_B/G_A = 1.93$. This equality taken in association with Eq. 42, in which α, β, θ_C, and λ_C are known, allows

an estimate of the two unknowns, G_A and G_B at 7.69×10^{-4} and 14.84×10^{-4} mho/cm^2, respectively, from which $R_A = 1{,}300\ \Omega\cdot\text{cm}^2$, $R_B = 674\ \Omega\cdot\text{cm}^2$, and further, $r_A = 3.94 \times 10^4\ \Omega\cdot\text{cm}$, and $r_B = 1.38 \times 10^4\ \Omega\cdot\text{cm}$. Note that, if the last tubule of this group were not discarded, the value of λ_C would be slightly lowered from 211 to 190 μm, θ_C would go up from 2,347 to 3,868 Ω·cm, but r_A and r_B would remain unaffected, 3.89×10^4 and $1.36 \times 10^4\ \Omega\cdot\text{cm}$, respectively.

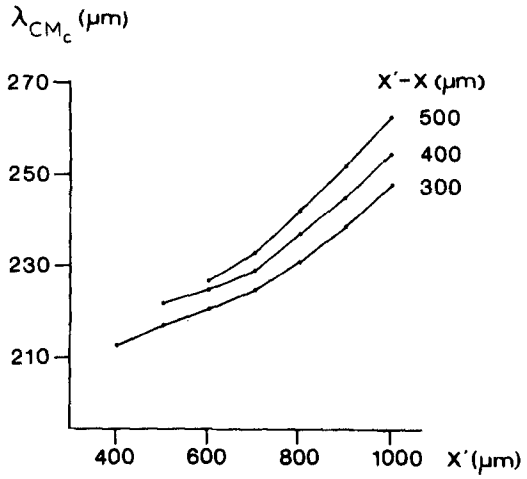

FIGURE 12. This drawing represents the value of λ_{CM_c}, corresponding to the theoretical cable described in Fig. 2, as a function of distance of the recording tips from the source and from one another. λ_{CM_c} (ordinate) was calculated according to the general equation

$$1/\lambda_{CM_c} = \left[\log V_{C_{(x')}} - \log V_{C_{(x)}}\right] / (x - x').$$

Each pair of log $V_{C_{(x)}}$ and x values was taken from Fig. 2 (upper curve). The abscissa indicates the position of the microelectrode more distant to the source. The three curves of the graph correspond (from top to bottom) to $x' - x$ distances of 500, 400, and 300 μm, respectively. The values of V_C are not experimental figures, they correspond to an ideal but hypothetical cable (resembling to the proximal tubule of *Necturus*) defined in Fig. 2. Thus, the computed variation of λ_{CM_c} represents a genuine change, and it cannot be ascribed to experimental errors.

DISCUSSION

Electrical Properties of the Proximal Tubule in Necturus

A quantative evaluation of the conductive properties of the proximal tubule in *Necturus* was carried out via two distinct theoretical approaches, using for each of them different sets of data. The results are in reasonable agreement with each other and may be summarized as follows: the resistance of the luminal membrane (per unit length) is almost three times greater than that of the basolateral membrane, 3.5×10^4 and $1.2 \times 10^4\ \Omega\cdot\text{cm}$. The shunt resistance

(per unit length) is slightly greater than that of the basolateral membrane, $1.7 \times 10^4\ \Omega \cdot cm$. The transcellular resistance (per unit length) is nearly three times as great as that of the shunt pathway. Taking into account the geometry of the tubule, the specific resistances of luminal membrane, basolateral membrane, and shunt pathway may be estimated at about 1,200, 600, and 600 $\Omega \cdot cm^2$, respectively. The various ratios relating specific resistances are of limited physiologic interest because the transepithelial ion transport (or current) is constant per unit of tubular length, not per unit of surface area, when the apical and basolateral membranes are considered in succession along the reabsorptive route.

The presently measured transepithelial specific resistance of the proximal tubule in the in vivo *Necturus* kidney (420 $\Omega \cdot cm^2$) is substantially higher than most recent estimates, according to which R_{TE} lies in the range from 40 (26, 28) to 70 (7) $\Omega \cdot cm^2$. Although such discrepancies cannot be accounted for on strictly scientific grounds, it should be pointed out that all artifacts conceivably arising during the determination of the luminal length constant (i.e., undetected leaks of current from lumen to interstitium) tend to decrease the experimentally determined λ_{LM_l} and, consequently, the resulting R_{TE}. It is also recalled that the figure of R_{TE} initially reported in the in vivo preparation by Windhager et al. (29) and refuted in subsequent publications was 650 $\Omega \cdot cm^2$. Furthermore, recent estimates of R_{TE} in the perfused *Necturus* kidney (not in the in vivo preparation) were 430 (19), 103 (27), and 255 $\Omega \cdot cm^2$ (9). In view of the large scatter of published R_{TE} values, over a range of one order of magnitude, on occasion by the same investigator, the most plausible interpretation is that the low estimates may be due to the existence of leaky impalements. From our data we raise the fundamental question as to what class of epithelia the proximal tubule of *Necturus* belongs to. If we accept the tentative notion that tight and leaky epithelia are opposed on the basis of their transepithelial resistance [the boundary being at or near 300 $\Omega \cdot cm^2$ (16)], then the present estimates of R_{TE} do not allow us to list the proximal tubule of *Necturus* with the leaky structures.

This study also provides the first direct measurements of individual cell membrane resistances. Their sum in series, i.e., the transcellular resistance (expressed as specific resistance), amounts barely to 2,000 $\Omega \cdot cm^2$. Previous estimates of R_{TC} range from 8,000 to 9,500 $\Omega \cdot cm^2$, in the in vivo (29) and in the perfused *Necturus* kidney (4), respectively. By comparison, R_{TC} in the proximal tubule of the rat is as low as 350 $\Omega \cdot cm^2$ (15). The present R_{TC} of $\sim$1,800 $\Omega \cdot cm^2$ cannot be compared with the figure of 7,900 $\Omega \cdot cm^2$, in vivo, reported by others (29), because neither current intensity I_0, nor the value of R_{PAR} (the single parameter measurable by the technique used in that study), nor the approximations used to convert R_{PAR} to the claimed R_{TC} of 7,900 $\Omega \cdot cm^2$, were mentioned. Our present figure of $R_{TC} \simeq 1{,}800\ \Omega \cdot cm^2$ is substantially lower than a previous approximation of 9,500 $\Omega \cdot cm^2$ by ourselves in the perfused *Necturus* kidney (4). It is also recalled that the epithelial core resistivity of 11,000 $\Omega \cdot cm$ in the in vitro preparation (4) was higher than present estimates of θ_C at 2,500–5,000 $\Omega \cdot cm$. Since in our previous work, the in vitro *Necturus* kidney was perfused with bicarbonate-free solutions (4), we suggest

that the prolonged removal of HCO_3 and/or other physiologic blood substrates from the peritubular perfusate result in a significant increase of cell membrane resistances and cell core resistivity; the latter is ascribed to augmentation of junctional resistance not to significant alteration of cytoplasmic resistivity.

Active Transport and Passive Electrical Properties of Epithelial Tissues

The presently measured figure of R_{TE} in the in vivo *Necturus* proximal tubule (420 $\Omega \cdot cm^2$), taken in association with recent findings from this laboratory of low transepithelial PDs (V_{TE}), in *Necturus*, i.e., of the order of -1 to -2 mV (2, 13, 14) allows an estimate of the passive transepithelial current flow (V_{TE}/R_{TE}) at 0.2–0.4 $\times$ 10^{-10} mol/$cm^2 \cdot s$. This figure may be compared with net transepithelial ion transport, determined from the half-time ($t_{1/2}$) of the oil split-drop technique. The $t_{1/2}$ of 30 min in the proximal tubule of *Necturus* (6, 7) is equivalent to transepithelial water flow of 3 $\times$ 10^{-8} $cm^3/cm \cdot s$; the method used to convert $t_{1/2}$ to water reabsorption is given in Gertz (18). Then, assuming the luminal Na concentration to be 0.1 mol/liter, we may easily evaluate the net transepithelial cation flux associated with isotonic water absorption at about 10^{-10} mol/$cm^2 \cdot s$. We infer that the net passive current occuring presumably across the shunt pathway (0.2–0.4 $\times$ 10^{-10} mol/$cm^2 \cdot s$) represents 20–40% of the net transepithelial ion transport (10^{-10} mol/$cm^2 \cdot s$). By contrast, the figures of $V_{TE} = -8$ mV and $R_{TE} = 40$ $\Omega \cdot cm^2$ (28) or those of $V_{TE} = -14$ mV and $R_{TE} = 70$ $\Omega \cdot cm^2$ (8) yield a transepithelial passive current of 200 $\mu A/cm^2$ (8) which is equivalent to about 20 $\times$ 10^{-10} mol/$cm^2 \cdot s$. According to these studies (8, 28) (based on very low estimates of R_{TE} and high values of V_{TE}), the net passive transepithelial ion transport would be greater than the net transepithelial transport by a factor of 20, an unreasonable conclusion.

An interspecies comparison of the calculated passive transepithelial ionic current (estimated by the V_{TE}/R_{TE} ratio) to the actual transepithelial transport rate (measured either directly or by the short-circuit technique), may be of some interest in the above argument (Fig. 13). The positive correlation observed between those parameters is consistent with the notion that high net (or active) transepithelial transport rates are associated with a large component of passive transepithelial transport, depending on the electrical properties of the epithelium. The data on the proximal tubule of *Necturus*, obtained from this laboratory fit the correlation depicted in Fig. 13, (O, bottom), as opposed to estimates provided by other studies (8, 28) (O, top). Although interspecies comparisons may be hardly taken to validate a particular set of data, the observed fit provides additional, yet indirect support to our findings.

Cable-to-Cable Interactions in Renal Tubules

An important finding of this study is that the determination of λ_{LM} and λ_{CM} by conventional techniques, in cylindrical epithelia such as renal tubules, may not provide reliable information on the conductive properties of the cable under consideration. The reason is that electrical interactions may arise between the two concentric cables consisting of the tubule lumen and the epithelial cells, resulting in distortions of the voltage attenuation curve in one

of the two cables. Although a variety of combinations may be thought of, we shall consider in general terms and very schematically, three particular patterns.

(*a*) $\lambda_D \gg \lambda_E$. This situation is encountered only in tight epithelia, but it is not necessarily present in all tight epithelia. The general equations (Eqs. 24 *a*, 24 *b*, 25 *a*, and 25 *b*) describing voltage attenuation in concentric cylindrical

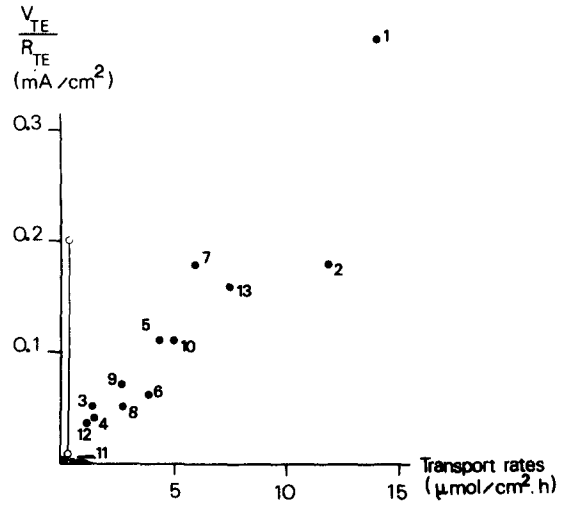

FIGURE 13. The calculated passive ionic current flowing across different epithelia (V_{TE}/R_{TE}, ordinate) is plotted as a function of net (or active) transepithelial ion transport (abscissa). Net transport was directly measured by tracer techniques; active transport was assumed to be equal to the short-circuit current. Each number represents a different tissue. Numbers 1–6 are taken from Frömter and Diamond (16). The tissues listed are (1) rat jejunum, (2) rat submandibular salivary gland, (3) frog skin, (4) toad urinary bladder, (5)turtle urinary bladder, (6) frog stomach, (7) rabbit ileum (23), (8) rabbit colon (24), (9) opercular skin of a teleost (12), (10) frog cornea (11), (11) cortical collecting duct of the rabbit (20), (12) thick ascending limb of Henle in the rabbit (10). The ordinate and abscissa of the proximal convoluted tubule of rabbit (22), 0.54 and 20, respectively, in line with the remainder, are not shown to avoid further reduction of the drawing. The proximal tubule of *Necturus* is represented by two ordinate points—the open circles connected by a vertical line. The upper point corresponds to the data obtained in other laboratories (8, 28), the lower one to the present study.

cables are simplified (as we did in the present study in *Necturus*) to the various expressions given by Eqs. 32–46. Two important consequences should be stressed again. First, the measured λ_{LM_l} is for all practical purposes identical to λ_D; it allows an estimate of r_{TE} (R_{TE}) by ordinary cable equations. Second, the slope of the measured λ_{CM_c} varies as a function of distance from the source, being very close to λ_E near the source and quite similar to λ_D ($\lambda_D \neq \lambda_E$) away from the source; as a result, the value of λ_{CM_c} in free-flow tubules cannot be used to assess R_{PAR} (and further R_{TC}) by conventional equations.

(*b*) $\lambda_E \gg \lambda_D$. This association is more likely to occur in leaky epithelia, i.e.,

when $R_S \ll R_{TC}$. Under these circumstances, simplification of the general equations (Eqs. 24 *a*, 24 *b*, 25 *a*, and 25 *b*) yields expressions quite different from those obtained in this paper for the proximal tubule of *Necturus*. Their main characteristics may be summarized as follows. The measurement of λ_{CM_c} with an intracellular point source may provide a good estimate of the sum of cell membrane resistances in parallel R_{PAR}, because in this situation it can be shown that $\lambda_{CM_c} \simeq \lambda_E$ and $\lambda_E = (r_{PAR}/\rho_C)^{1/2}$. Conversely luminal injection of current is likely to generate an "equivalent intraepithelial source" near the actual source, resulting in voltage spread along the epithelium and having a slope λ_{CM_l} similar to λ_{CM_c}. The slope of the luminal cable, λ_{LM_l} will be distorted by intraepithelial voltage attenuation. Thus, the transepithelial resistance r_{TE} (R_{TE}) cannot be determined with accuracy from λ_{LM_l} using ordinary cable equations. Appropriate expressions, derived from the general equations (Eqs. 24 and 25), are necessary to evaluate r_{TE}.

(*c*) The third variety is defined by λ_E and λ_D values very close to each other. It may occur in both tight and leaky epithelia. The prerequisite condition is that large communications between luminal and epithelial cables cause them to behave as an electrical syncitium, i.e., $R_B \gg R_S > R_A$. In this situation the apparent slopes of voltage attenuation λ_{CM} and λ_{LM} are quite close to each other and hardly distinguishable by experimental means, irrespective of source localization. Apart from the determination of R_B in oil-filled tubules, which is not subject to interactions, there is no method to assess R_A and R_S using ordinary cable equations. Furthermore, one of the premises of our theoretical analysis (the postulate of independent luminal and epithelial cables) is not warranted in this case in which the two cables are electrically indistinguishable: Eqs. 24 and 25 become then inadequate to describe voltage attenuation in the two companion cables. The ratio of the various resistive barriers may be estimated by measuring the ratio of voltages from lumen to interstitium using an axial luminal wire to inject current (28) and/or by the simultaneous study of transepithelial and cell potential changes occuring during changes of luminal and peritubular perfusate composition (1, 17).

The mathematical treatment of voltage attenuation in double cables was performed by J. Teulon and A. Edelman.

This study was supported by grants from the Institut National de la Santé et de la Recherche Médicale and the Delegation Générale à la Recherche Scientifique et Technique.

Received for publication 28 November 1978.

REFERENCES

1. ANAGNOSTOPOULOS, T. 1973. Biionic potentials in the proximal tubule of *Necturus* kidney. *J. Physiol. (Lond.).* **233:**375–394.
2. ANAGNOSTOPOULOS, T. 1975. Anion permeation in the proximal tubule of *Necturus* kidney: the shunt pathway. *J. Membr. Biol.* **24:**365–380.
3. ANAGNOSTOPOULOS, T. 1977. Electrophysiological study of the peritubular membrane in the proximal tubule of *Necturus*: effect of inorganic anions and SCN^-. *J. Physiol. (Lond.)* **267:** 89–111.
4. ANAGNOSTOPOULOS, T., and E. VELU. 1974. Electrical resistance of cell membranes in *Necturus* kidney. *Pflügers Arch. Eur. J. Physiol.* **346:**327–339.

5. BENTZEL, C. J. 1972. Proximal tubule structure-function relationships during volume expansion in *Necturus*. *Kidney Int.* **2**:324–335.
6. BENTZEL, C. J., T. ANAGNOSTOPOULOS, and H. PANDIT. 1970. *Necturus* kidney: its response to effects of isotonic volume expansion. *Am. J. Physiol.* **218**:205–213.
7. BOULPAEP, E. L. 1972. Permeability changes of the proximal tubule of *Necturus* during saline loading. *Am. J. Physiol.* **222**:517–531.
8. BOULPAEP, E. L. 1976. Electrical phenomena in the nephron. *Kidney Int.* **9**:88–102.
9. BOULPAEP, E. L. 1977. Electrophysiological study of the *Necturus* proximal tubule: effects of organic substrates and segmental heterogeneity. *In* Electrophysiology of the Nephron, T. Anagnostopoulos, editor. INSERM Editions, Paris. Vol. 67. 127–134.
10. BURG, M. B., and N. GREEN. 1973. Function of the thick ascending limb of Henle's loop. *Am. J. Physiol.* **224**:659–668.
11. CANDIA, O. A., P. J. BENTLEY, and P. I. COOK. 1974. Stimulation by amphotericin B of active Na transport across amphibian cornea. *Am. J. Physiol.* **226**:1438–1444.
12. DEGNAN, K. J., K. J. KARNAKY, JR., and J. A. ZADUNAISKY. 1977. Active chloride transport in the in vitro opercular skin of a teleost (*Fundulus heteroclitus*), a gill-like epithelium rich in chloride cells. *J. Physiol. (Lond.)*. **271**:155–191.
13. EDELMAN, A., and T. ANAGNOSTOPOULOS. 1976. Transepithelial potential difference in the proximal tubule of *Necturus* kidney. *Pflügers. Arch. Eur. J. Physiol.* **363**:105–111.
14. EDELMAN, A., and T. ANAGNOSTOPOULOS. 1978. Further studies on ion permeation in proximal tubule of *Necturus* kidney. *Am. J. Physiol.* **235**:F89–F95.
15. FRÖMTER, E. 1976. Magnitude and significance of the paracellular shunt path in rat kidney proximal tubule. *In* Intestinal Permeation. M. Kramer and F. Lauterbach, editors. Excerpta Medica, Amsterdam. 393–405.
16. FRÖMTER, E., and J. DIAMOND. 1972. Route of passive ion permeation in epithelia. *Nat. New Biol.* **53**:9–13.
17. FRÖMTER, E., C. W. MÜLLER, and T. WICK. 1971. Permeability properties of the proximal tubular epithelium of the rat kidney studied with electrophysiological methods. *In* Electrophysiology of Epithelial Cells. G. Giebisch, editor. F. K. Schattauer Verlag, Stuttgart. 119–146.
18. GERTZ, K. H. 1965. On the glomerular tubular balance in the rat kidney. *Pflügers Archiv Gesamte Physiol. Menschen Tiere.* **285**:360–372.
19. GRANDCHAMP, A., and E. L. BOULPAEP. 1974. Pressure control of sodium reabsorption and intercellular backflux across proximal kidney tubule. *J. Clin. Invest.* **54**:69–82.
20. HELMAN, S. I., and R. G. O'NEIL. 1977. Model of active transepithelial Na and K transport of renal collecting tubules. *Am. J. Physiol.* **233**:F559–F571.
21. JACK, J. J. B., D. NOBLE, and R. W. TSIEN. 1975. Electric Current Flow in Excitable Cells. Clarendon Press, Oxford. 31
22. LUTZ, M. D., J. CARDINAL, and M. B. BURG. 1973. Electrical resistance of renal proximal tubule perfused in vitro. *Am. J. Physiol.* **225**:729–734.
23. NELLANS, H. N., R. A. FRIZZELL, and S. G. SCHULTZ. 1975. Effect of acetazolamide on sodium and chloride transport by the in vivo rabbit ileum. *Am. J. Physiol.* **228**:1808–1814.
24. SCHULTZ, S. G., R. A. FRIZZELL, and H. N. NELLANS. 1977. Active sodium transport and the electrophysiology of rabbit colon. *J. Membr. Biol.* **33**:351–384.
25. SHIBA, H. 1971. Heavisides "Bessel cable" as an electric model for flat simple epithelial cells with low resistive junctional membranes. *J. Theor. Biol.* **30**:59–68.
26. SPRING, K. R. 1973. Current-induced voltage transients in *Necturus* proximal tubule. *J. Membr. Biol.* **13**:299–322.

27. SPRING, K. R. 1977. Electrical properties of the *Necturus* proximal tubule. *In* Electrophysiology of the Nephron. T. Anagnostopoulos, editor. INSERM Editions, Paris. Vol. 67. 161–182.

28. SPRING, K. R., and C. V. PAGANELLI. 1972. Sodium flux in *Necturus* proximal tubule under voltage clamp. *J. Gen. Phyisol.* **60**:181–201.

29. WINDHAGER, E. E., E. L. BOULPAEP, and G. GIEBISCH. 1967. Electrophysiological studies on single nephrons. *Proc. Int. Congr. Nephrol.* **3**:35–47.